arXiv:1709.05419v2 [hep-ph] 25 Jan 2018

Physics of Elementary Particles and Atomic Nuclei. Theory

Threshold Collision Energy of the QCD Phase Diagram Tricritical Endpoint

K. A. Bugaev[a1], R. Emaus[b], V. V. Sagun[a,c] A. I. Ivanytskyi[a], L. V. Bravina[b], D. B. Blaschke[d,e,f], E. G. Nikonov[g], A. V. Taranenko[f], E. E. Zabrodin[b,f,h], G. M. Zinovjev[a]

[a] Bogolyubov Institute for Theoretical Physics, Metrologichna str. 14^B, Kiev 03680, Ukraine

[b] Department of Physics, University of Oslo, PB 1048 Blindern, N-0316 Oslo, Norway

[c] CENTRA, Instituto Superior Técnico, Universidade de Lisboa, Av. Rovisco Pais 1, 1049-001 Lisboa, Portugal

[d] Institute of Theoretical Physics, University of Wroclaw, pl. M. Borna 9, 50-204 Wroclaw, Poland

[e] Bogoliubov Laboratory of Theoretical Physics, JINR Dubna, Joliot-Curie str. 6, 141980 Dubna, Russia

[f] National Research Nuclear University "MEPhI" (Moscow Engineering Physics Institute), Kashirskoe Shosse 31, 115409 Moscow, Russia

[g] Laboratory for Information Technologies, JINR, Joliot-Curie str. 6, 141980 Dubna, Russia

[h] Skobeltzyn Institute of Nuclear Physics, Moscow State University, 119899 Moscow, Russia

Using the most advanced formulation of the hadron resonance gas model we analyze the two sets of irregularities found at chemical freeze-out of central nuclear-nuclear collisions at the center of mass energies 3.8-4.9 GeV and 7.6-9.2 GeV. In addition to previously reported irregularities at the collision energies 4.9 GeV and 9.2 GeV we found sharp peaks of baryonic charge density. Also we analyze the collision energy dependence of the modified Wroblewski factor and the strangeness suppression factor. Based on the thermostatic properties of the mixed phase of a 1-st order phase transition and the ones of the Hagedorn mass spectrum we explain, respectively, the reason of observed chemical equilibration of strangeness at the collision energy 4.9 GeV and above 8.7 GeV. It is argued that the both sets of irregularities possibly evidence for two phase transitions, namely, the 1-st order transition at lower energy range and the 2-nd order transition at higher one. In combination with a recent analysis of the light nuclei number fluctuations we conclude that the center of mass collision energy range 8.8-9.2 GeV may be in the nearest vicinity of the QCD tricritical endpoint. The properties of the phase existing between two phase transitions are revealed and discussed.

PACS: 25.75.−q, 25.75.Nq

[1]E-mail: bugaev@fias.uni-frankfurt.de

Introduction

Theoretical and experimental searches for the (tri)critical endpoint ((3)CEP) of the quantum chromodynamics (QCD) phase diagram form one of the most important directions of physics of heavy ion collisions [1, 2]. Despite the claims that the QCD CEP parameters can be extracted from the RHIC data [3], the real situation is not so clear [4]. In part, such a situation exists because the rigorous and reliable definition of finite volume analog of (3)CEP does not exist. In our opinion, therefore, the question is not whether the work [5] can justify the finite size scaling for the isothermal compressibility as it is assumed in [3] or for the isentropic compressibility as its is argued in [4], but whether there is sufficient experimentally established signals of the (3)CEP formation. Furthermore, we are sure that to safely locate the threshold collision energy of the (3)CEP one needs a simultaneous match of thermodynamical, statistical and hydrodynamical signals of its formation.

Recently the thermodynamical and hydrodynamical signals of the mixed quark-gluon-hadron phase formation were revealed [6, 7] from the analysis of different irregularities observed at chemical freeze-out (CFO) [8–10]. Moreover, such signals were observed at two ranges of the center-of-mass collision energies, namely $\sqrt{s_{NN}} \simeq 3.8 - 4.9$ GeV and $\sqrt{s_{NN}} \simeq 7.6 - 9.2$ GeV [6, 7, 10]. The thermodynamic signals include two sharp peaks of the trace anomaly $\delta = \frac{(\epsilon - 3p)}{T^4}$ (here ϵ, p and T denote, respectively, the energy density of the system, its pressure and temperature) observed at $\sqrt{s_{NN}} = 4.9$ GeV and $\sqrt{s_{NN}} = 9.2$ GeV, while the hydrodynamic signals consist of the highly correlated quasi-plateaus in the collision energy dependence of the entropy per baryon, total pion number per baryon, and thermal pion number per baryon which were found at the two ranges of the center-of-mass collision energies discussed above [6, 7]. Thermodynamical and hydrodynamical signals in the low collision energy region can be easily interpreted since they can be related with each other via the generalized shock adiabat model [11, 12] which shows that there is one-to-one correspondence between the peak of δ at CFO and the peak of δ at the shock adiabat [6, 7]. Moreover, at CFO the low energy signals are accompanied by the strong jumps of the pressure p and the effective number of degrees of freedom p/T^4 [6–8]. In contrast to these findings, the high energy signals are less pronounced and, hence, their interpretation is not straightforward [6, 7, 10] and, therefore, one needs additional analysis of the collision energy range $\sqrt{s_{NN}} \simeq 7.6 - 9.2$ GeV.

In a recent work on the analysis of critical fluctuations of light nuclei [13] at CFO it was argued that at the collision energy $\sqrt{s_{NN}} = 8.8$ GeV the QCD matter has strongest fluctuations and, hence, during its evolution this matter passes through the CEP. This work puts forward a strong argument in favor of the hypothesis that at the vicinity of the point $\sqrt{s_{NN}} = 8.8$ GeV, i.e. almost at the location of the second peak of trace anomaly δ, there occurs another phase transformation. Moreover, the work [13] concludes that this is a vicinity of CEP, i.e. it has to be a 2-nd order phase transition. Thus, in addition to the thermodynamic and hydrodynamic signals of a possible phase transformation at the collision energy range $\sqrt{s_{NN}} \simeq 7.6 - 9.2$ GeV [6, 7, 10] the work [13], first of all, gives an additional and independent evidence in favor of such a transformation and, moreover, it provides us with the necessary statistical (fluctuation) signal. However, in combination with the previous findings on the signals of 1-st order phase transition at the collision energies $\sqrt{s_{NN}} \simeq 4.3 - 4.9$ GeV [6, 7, 10] one should conclude that these are

the signals of two phase transitions and, therefore, at the vicinity of collision energies $\sqrt{s_{NN}} \simeq 8.8 - 9.2$ GeV there may exist not a CEP, but a 3CEP. It should be stressed that this is highly nontrivial conclusion, since neither the lattice QCD nor the QCD inspired field-theoretical models can presently tell us for sure whether QCD has the CEP or 3CEP.

Furthermore, if we observe the signals of two phase transitions there are two basic questions related to this fact: (I) can one determine which of these transitions is deconfinement and which one is the chiral symmetry restoration? and (II) what kind of phase can be probed at the collision energies $\sqrt{s_{NN}} \simeq 4.9 - 8.8$ GeV? The present work is an attempt to formulate the proper answers to these two major questions.

The work is organized as follows. In the next section we present the details of hadron resonance gas model and the fitting procedure of hadronic multiplicities. Section 3 is devoted to an analysis of new irregularities at CFO. In Section 4 we discuss the properties of explicit thermostat and apply them to explain the strangeness equilibration observed at the collision energy $\sqrt{s_{NN}} = 4.9$ GeV. Also in this section we estimate the number of degrees of freedom of a phase possibly formed at $\sqrt{s_{NN}} \simeq 4.9 - 8.8$ GeV. The equation of state of (almost) massless particles with the relativistic treatment of hard-core repulsion is analyzed in Section 5. Our conclusions are summarized n Section 6.

Analysis of hadron multiplicities

First we perform the cross-check of the previously obtained results on the irregularities at CFO [6,7,10]. For this purpose we employ the newest version of the hadron resonance gas model (NHRGM) [14–16] which allows us to safely go beyond the usual Van der Waals approximation for the multicomponent case, i.e. for several different hard-core radii of hadrons. Also below we reveal the new irregularities and give their explanation based on the hypothesis of existence of two phase transitions.

The new key element of the NHRGM is an inclusion of the surface tension which is generated by the hard-core repulsion. Therefore, this equation of state is called the induced surface tension one. For the system with multicomponent hard-core repulsion in the grand canonical ensemble this equation of state is given by the system of two coupled equations

$$p = \sum_n p_n^{id}\left(T, \mu_n - pV_n - \Sigma S_n\right), \tag{1}$$

$$\Sigma = \sum_n R_n\, p_n^{id}(T, \mu_n - pV_n - \alpha\Sigma S_n), \tag{2}$$

where the sums are running over all particles (and antiparticles) with the chemical potentials μ_n, the hard-core radii R_n, the proper volumes $V_n = \frac{4}{3}\pi R_n^3$ and the proper surfaces $S_n = 4\pi R_n^2$. Here $p_n^{id}(T, \mu_n)$ denotes the partial pressure of the point-like particles of sort n with the degeneracy g_n and the mass m_n which in case of the Boltzmann statistics is

$$p_n^{id}(T, \nu) = g_n \int \frac{d\mathbf{k}}{(2\pi^3)} \frac{k^2}{3\, E_n(k)} e^{\frac{\nu - E_n(k)}{T}}. \tag{3}$$

Here $E_n(k) = \sqrt{\vec{k}^2 + m_n^2}$ is the energy of particle with the 3-momentum $\vec{k}$ and ν is the effective chemical potential.

In the grand canonical ensemble the one component Van der Waals equation of state (EoS) [8,17,18] can be obtained from the pressure of ideal gas, classical or quantum, by the modification of the chemical potential as $\mu_1 \to \mu_1 - 4V_1 p$ [19]. In the one component NHRGM the free energy associated with the excluded volume of particle $-4V_1 p$ is split up into a sum of the volume part $-V_1 p$, which is proportional to the pressure p, and the surface part $-S_1\Sigma$, which is proportional to the induced surface tension coefficient Σ (here S_1 is the proper surface of particle having the hard-core radius R_1). Such a splitting allows one not only to account for the second virial coefficient, but also to reproduce the third and the fourth ones of the gas of hard-spheres of the radius R_1 with a good accuracy [14,15]. The system (1) and (2) is a generalization of such an approach to a multicomponent case. The parameter $\alpha > 1$ switches between the excluded-volume and the proper-volume regimes. Numerical analysis [15] shows that for $\alpha = 1.245$ the system (1) and (2) correctly reproduces the one component [20] and multicomponent [21] versions of the well-known Carnahan-Starling EoS up to the packing fractions $\eta = \sum\limits_{n=1} V_n \rho_n \leq 0.22 - 0.24$ (here ρ_n is the particle number density of hadron species n). Note that the Carnahan-Starling EoS and its multicomponent version [21] are well-known in the theory of simple liquids since they are able to reproduce the EoS of hard spheres up to its transition to a liquid state [22,23].

The particle density of hadrons of sort n,

$$\rho_n \equiv \frac{\partial p}{\partial \mu_n} = \frac{1}{T} \cdot \frac{p_n\, a_{22} - \Sigma_n\, a_{12}}{a_{11}\, a_{22} - a_{12}\, a_{21}}\,, \tag{4}$$

is expressed in terms of the auxiliary coefficients

$$a_{11} = 1 + \sum_n V_n \frac{p_n}{T}\,, \quad a_{12} = \sum_n S_n \frac{p_n}{T}\,, \tag{5}$$

$$a_{21} = \sum_n V_n \frac{\Sigma_n}{T}\,, \quad a_{22} = 1 + \sum_n \alpha S_n \frac{\Sigma_n}{T}\,. \tag{6}$$

At CFO the ratio of total hadronic multiplicities of sorts i and j is given by

$$R_{ij} \equiv \frac{N_i^{tot}}{N_j^{tot}} = \frac{\rho_i + \sum_{l\neq i} \rho_l\, Br_{l\to i}}{\rho_j + \sum_{l\neq j} \rho_l\, Br_{l\to j}}\,. \tag{7}$$

This expression accounts for the hadrons which appear in strong decays of resonances with the branching ratios $Br_{l\to j}$. The total chemical potential of hadron of the sort n is $\mu_n = Q_n^B \mu_B + Q_n^S \mu_S + Q_n^{I3} \mu_{I3}$ and it depends on the baryonic chemical potential μ_B, the strange chemical potential μ_S, the isospin third projection chemical potential μ_{I3} and the corresponding charges Q_n^B, Q_n^S, Q_n^{I3} of this hadron. More details on the NHRGM can be found in [15].

Similarly to [10], here we fit the high quality experimental multiplicity ratios measured at AGS for $\sqrt{s}_{NN} = 2.7, 3.3, 3.8, 4.3, 4.9$ GeV [24–32], the NA49 data measured at SPS energies $\sqrt{s}_{NN} = 6.3, 7.6, 8.8, 12.3, 17.3$ GeV [33–41] and the STAR data measured at

RHIC energies $\sqrt{s}_{NN} = 9.2, 62.4, 130, 200$ GeV [42]. These experimental data allow us to construct 111 independent ratios measured at 14 collision energies [8, 18]. In order to verify the stability of the results on the new signals of phase transition between the hadron and quark gluon matters found in [10] with the help of the HRGM based on the Van der Waals approximation and to improve the description of (anti)Λ-hyperons and (anti)protons we added 10 experimental data points of the Λ/p ratio (on its exclusive role see a discussion in [7]). Although the Λ/p ratio can be expressed via other ratios, i.e. it is dependent, but at AGS and SPS energies this ratio has rather small error bars compared to other ratios and this is important for the fit stability [10]. Hence, in present work we analyze 121 ratios.

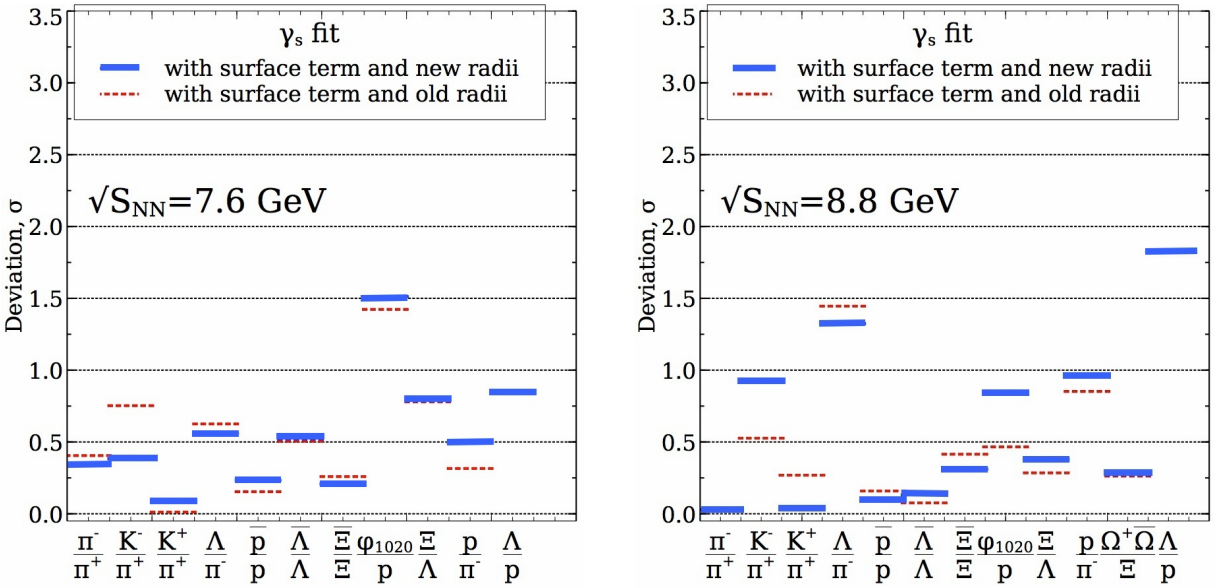


Fig. 1. Deviations of theoretically predicted hadronic yield ratios from experimental values in units of experimental error σ are shown for the center of mass collision energies $\sqrt{s_{NN}} = 7.6$ GeV and $\sqrt{s_{NN}} = 8.8$ GeV. Blue lines correspond to the IST EoS fit, while the red lines correspond to the original HRGM fit [15].

In addition, compared to works [10, 14, 15] we used a new set of global fitting parameters to minimize the mean square deviation $\chi^2 = \sum_{p=1}^{121} \frac{(R_p^{theor} - R_p^{exp})^2}{\sigma_p^2}$, where the experimental ratios are denoted as R_p^{exp}, the theoretical ones as R_p^{theor} and the summation is carried out over all data points with the weights defined by the experimental error σ_p. The minimization of χ^2 showed that compared to previous results [7, 10, 15] the values of local fitting parameters T, μ_B, μ_{I3} and γ_s are practically the same. We found the best description of the hadronic multiplicity ratios for the hard-core radius of pions $R_\pi = 0.2$ fm, (anti)Λ-hyperons $R_\Lambda = 0.05$ fm, (anti)protons $R_p = 0.37$ fm, other baryons $R_b = 0.4$ fm and other mesons $R_m = 0.43$ fm. This set of radii, i.e. the new radii afterwards, corresponds to a global minimum of $\chi^2/dof = 65.42/65 \simeq 1.01$ which

provides practically the same quality of fit as the set of global fitting parameters reported in [10, 15].

The set of old radii fitted in [15] provided $\chi^2_1/dof = 57.099/55 \simeq 1.038$ and it included the hard-core radii of pions R_π=0.15 fm, kaons R_K=0.395 fm, Λ-hyperons R_Λ=0.085 fm, baryons R_b=0.365 fm and mesons R_m=0.42 fm. Comparing these two sets of hard-core radii and their fit quality one concludes that there are slight changes only which lead to little improvements. This can be seen from the ratios shown in Figs. 1 and 2. Therefore, our main conclusion is that the results previously obtained within the multicomponent Van der Waals EoS are almost unchanged and, hence, there is no need to revise the signals of phase transitions suggested earlier in [6, 7, 10].

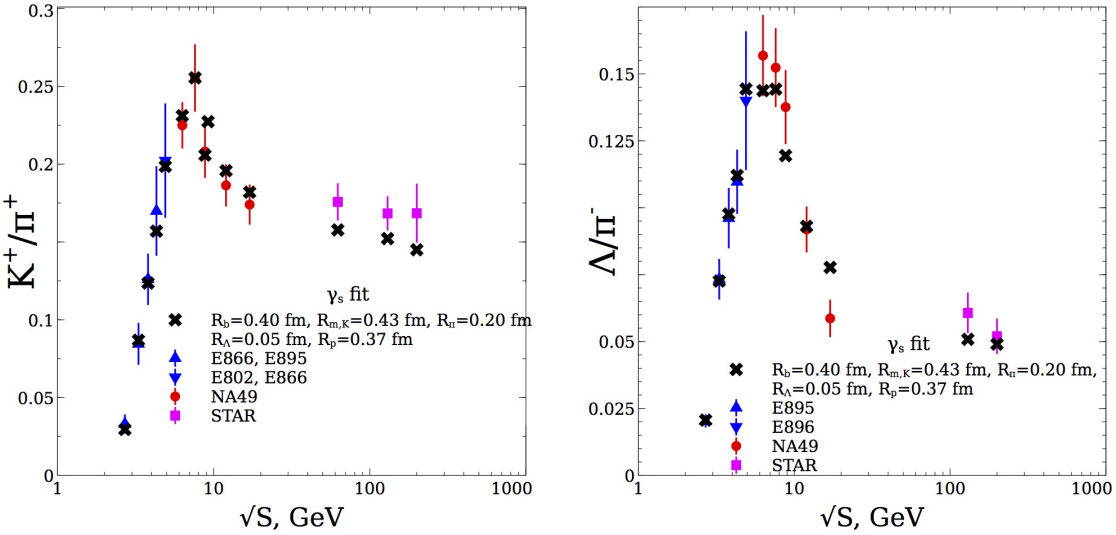


Fig. 2. The fit results obtained by the NHRGM with the new radii. Left panel: $\sqrt{s_{NN}}$ dependence of K^+/π^+. Right panel: $\sqrt{s_{NN}}$ dependence of Λ/π^-.

Concerning the small values of the hard-core radii of pions and (anti)Λ hyperons we would like to mention that these radii are an effective ones. It is possible that small value of the pion hard-core radius is a reflection of necessity to account for its relativistic nature at temperatures above 120 MeV [43, 44]. On the other hand the small hard-core radius of (anti)Λ hyperons may reflect some subtleties of their interaction with hadronic medium. Hence, we hope that their values provide an important information for microscopic models of hadronic interaction which will have to explain our results.

New irregularities at CFO

Further results concerning the trace anomaly and baryon density are shown in Fig. 3. From the both panels of this figure one can see that each peak of the trace anomaly δ is accompanied by a strong peak of the total baryonic density $\rho_B = \frac{\partial p}{\partial \mu_B}$. Moreover, the

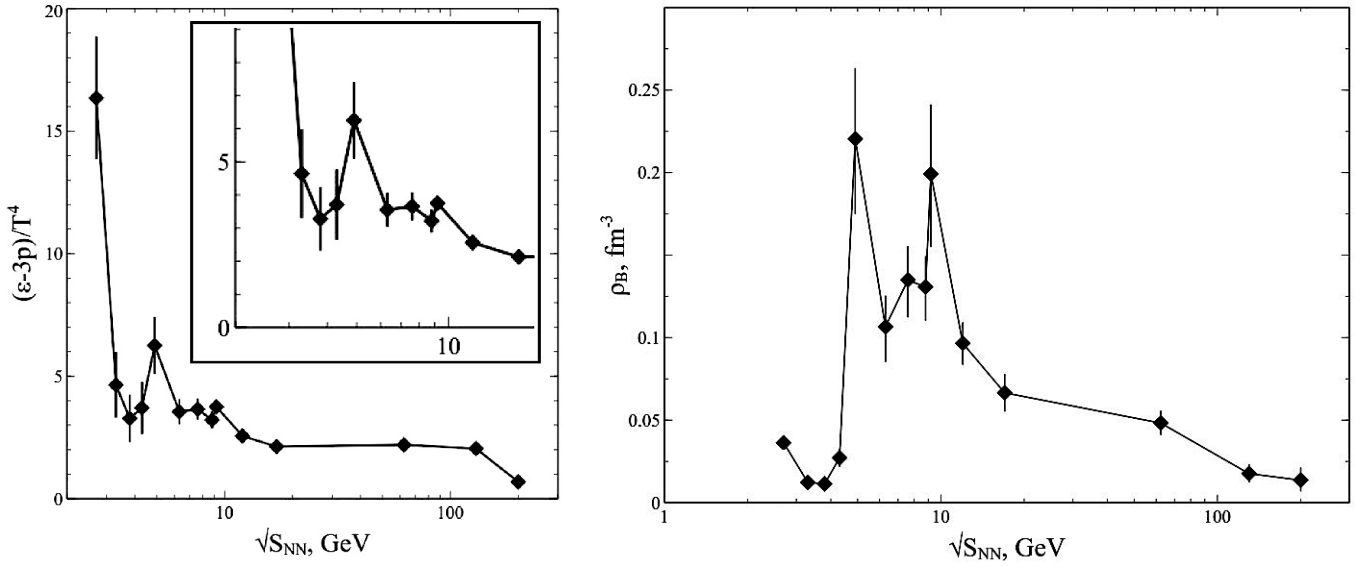


Fig. 3. Collision energy dependence of the trace anomaly δ (left) and baryonic charge density ρ_B (right) at CFO. The points are connected in order to guide the eye.

trace anomaly peak at $\sqrt{s_{NN}} = 9.2$ GeV has a small amplitude, while its counterpart in the baryonic density has a large amplitude accompanied by small error bars making this peak quite pronounced.

From the left panel of Fig. 4 one can see even more dramatic changes in the collision energy dependence of the modified Wroblewski factor λ_s [45] which we define as

$$\lambda_s \equiv \frac{2\sum\limits_n (N_n^S + N_n^{\bar{S}})\rho_n}{\sum\limits_n (N_n^u + N_n^{\bar{u}} + N_n^d + N_n^{\bar{d}})\rho_n}\,, \tag{8}$$

where in the numerator N_n^S and $N_n^{\bar{S}}$ denote, respectively, the number of strange valence quarks and antiquarks in the hadron of sort n, whereas N_n^u and N_n^d in the denominator denote, respectively, the number of u and d quarks in it (apparently, $N_n^{\bar{u}}$ and $N_n^{\bar{d}}$ play the same role for antiquarks). Note that the denominator in Eq. (8) differs from the traditional Wroblewski factor [45] because it accounts for a whole number of u and d valence quarks and antiquarks, and not only the ones which are paired to their valence antiquarks (quarks).

As one can see from Fig. 4 the factor λ_s demonstrates a jump right in the collision energy region which is associated with the mixed phase formation, i.e. for $\sqrt{s_{NN}} = 4.3 - 4.9$ GeV, and in addition it shows a change of slope at $\sqrt{s_{NN}} > 7.6$ GeV. Note that a similar behavior was found in [10] for the ratio $\frac{\Delta\Lambda}{\Delta p} = \frac{\Lambda - \bar{\Lambda}}{p - \bar{p}}$ and we confirm that in the present analysis it behaves similarly. The found collision energy dependence of λ_s further supports the hypothesis of Ref. [10] that such a behavior of $\frac{\Delta\Lambda}{\Delta p}$ and, hence, of λ_s is an indicator of two phase transformations. Indeed, the observed jump of these

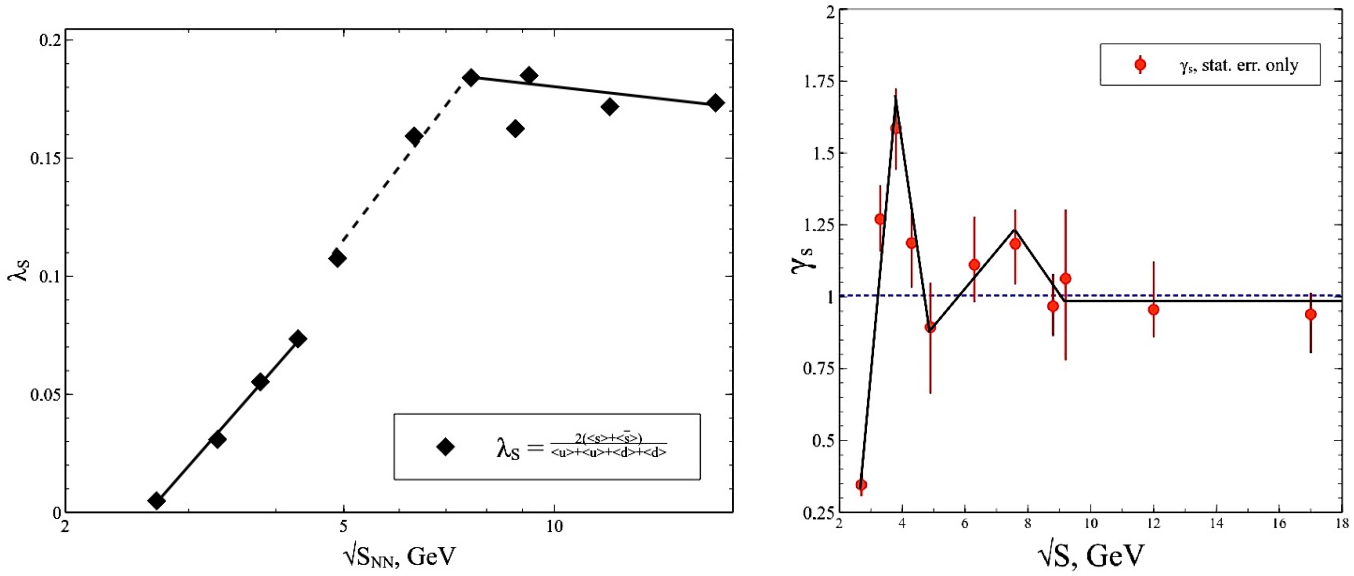


Fig. 4. Left panel: Collision energy dependence of the modified Wroblewski factor λ_s. Diamonds show the NHRGM description of experimental data. At and above $\sqrt{s_{NN}} = 7.6$ GeV there is a saturation of λ_s. Right panel: Collision energy dependence of the strangeness suppression factor γ_s found by the NHRGM clearly indicates the strangeness equilibrium dale at $\sqrt{s_{NN}} = 4.9$ GeV. The points are connected in order to guide the eye.

ratios is located in the collision energy range of the mixed phase formation (i.e. it is a 1-st order phase transition), then a change of their slope at $\sqrt{s_{NN}} > 7.6$ GeV can be naturally associated with a weak 1-st order or a 2-nd order phase transition.

The collision energy behavior of the strangeness suppression factor γ_s [46] shown in the right panel of Fig. 4 demonstrates more complicated dependence. Here one can see two peaks for $\sqrt{s_{NN}} < 8.8$ GeV which evidence about the strangeness enhancement (over-saturation) and the strangeness equilibrium dale at $\sqrt{s_{NN}} = 4.9$ GeV. At and above $\sqrt{s_{NN}} \geq 8.8$ GeV one observes a chemical equilibration of strange charge, since $\gamma_s = 1$. One might think that compared to the γ_s peak at $\sqrt{s_{NN}} = 3.8$ GeV the smaller one seen at $\sqrt{s_{NN}} = 7.6$ GeV is not statistically significant. However, a thorough analysis of two alternative approaches to describe the chemical non-equilibrium of strangeness performed in [47] shows that the γ_s peak in the vicinity of $\sqrt{s_{NN}} = 7.6$ GeV exists practically unmodified (see the upper panel of Fig. 2 in [47]). At the same time the regime of reaching the strangeness chemical equilibrium, i.e. $\gamma_s = 1$, at $\sqrt{s_{NN}} \geq 8.8$ GeV is also observed in [47].

Based on this discussion we can further refine a hypothesis on the cause of chemical equilibrium of strange charge in central nuclear collisions at the collision energy $\sqrt{s_{NN}} \geq 8.8$ GeV formulated in [15]. In our opinion, the most natural explanation of this phenomenon is that at $\sqrt{s_{NN}} \geq 8.8$ GeV there appeared the quark-gluon bags with the exponential mass spectrum proposed by R. Hagedorn [48]. As it was predicted in [49]

and shown numerically in [50–52], the exponential mass spectrum acts as a perfect thermostat and a perfect particle reservoir. In other words, all particles which appear from such bags at their hadronization will be born in a state of full thermal and chemical equilibrium [48, 50–52].

Furthermore, an existence of two peaks of γ_s strongly enhances the hypothesis about existence of two phase transformations. Indeed, since the right slope of the higher peak contains the region of the 1-st order phase transition at $\sqrt{s_{NN}} = 4.3 - 4.9$ GeV, then it is naturally to assume that the right slope of the lower peak also contains the phase transition region. Moreover, from Fig. 4 one can see that the end of the 1-st order phase transition is shifted on 1.1 GeV to a higher collision energy than the peak existing at $\sqrt{s_{NN}} = 3.8$ GeV. Then in accordance with our hypothesis the end of the other phase transition should be also shifted on about 1.1 GeV to a higher collision energy than the peak at $\sqrt{s_{NN}} = 7.6$ GeV, i.e. one would expect it at $\sqrt{s_{NN}} \simeq 8.7$ GeV. Thus, again we independently arrive to the same conclusion as from the analysis of the trace anomaly and the baryonic density peaks that the vicinity of $\sqrt{s_{NN}} \simeq 8.8 - 9.2$ GeV corresponds to a phase transformation. Since this conclusion is based on the assumption that the 1-st order phase transition can be reached at $\sqrt{s_{NN}} = 4.3 - 4.9$ GeV, then it is logically to expect that QCD has a 3CEP and it is located close to the collision energy range $\sqrt{s_{NN}} \simeq 8.8 - 9.2$ GeV. Thus, quite independently to Ref. [13] we came to a similar conclusion about the endpoint, but, in contrast to [13], we consider it as the 3CEP.

Note that the collision energy $\sqrt{s_{NN}} \simeq 8.8$ GeV as the onset of deconfined phase appears not only in Ref. [13]. Thus, in Ref. [53] it was shown that the horn in K^+/π^+ ratio can be naturally explained, if one assumes that the partonic phase, or the quark gluon plasma (QGP) production threshold is $\sqrt{s_{NN}} \simeq 8.8$ GeV. Note that we came to a similar conclusion above on the basis of the Hagedorn thermostat hypothesis. But now we are facing a question, if the QGP is formed in heavy ion collisions at $\sqrt{s_{NN}} \simeq 8.8$ GeV, then what kind of phase transition occurs at lower collision energies $\sqrt{s_{NN}} = 4.3 - 4.9$ GeV? From the discussion above it is evident that such a phase cannot consist from the bags of QGP which are filled with the quarks and gluons, otherwise one would find $\gamma_s = 1$.

Strangeness equilibrium dale and mixed phase as an explicit thermostat

Before discussing the possible interpretations of the above results, we would like to reinforce our arguments about the mixed phase formation at $\sqrt{s_{NN}} = 4.3 - 4.9$ GeV. Using the thermostatic properties of the mixed phase of the 1-st order phase transition [49] below we would like to explain the appearance of the strangeness equilibrium dale, i.e. $\gamma_s \simeq 1$, at $\sqrt{s_{NN}} = 4.9$ GeV. In [49] the examples of the explicit thermostat and explicit particle reservoir were discussed and it was argued that under the constant pressure condition the mixed phase of the 1-st order phase transition, i.e. two pure phases being in a thermal and chemical equilibrium with each other, represent both thermostat and particle reservoir as long as it has enough energy resources to keep a constant temperature. In other words, under the constant pressure condition an explicit thermostat keeps a constant temperature despite transmitting out (in) some amount of heat. The latter only changes the volume fractions of two phases: the phase with

higher heat capacity (for definiteness, a liquid) condenses a certain amount of gas under external cooling or it partly evaporates into a gas under external heating. Apparently, for finite systems the amount of imparted heat is also finite and depends on the masses of both phases and their heat capacities. Similarly, one can add or remove some amount of each phase, but under the constant pressure condition the system will continue to keep a constant temperature and a full chemical equilibrium, i.e. the equal values of chemical potentials for both pure phases. For our discussion it is important that up to some maximal value any amount of the removed phase, namely the gas of hadrons, for definiteness, will be, by definition, in a full chemical and thermal equilibrium with the mixed phase. Again the maximal amount of removed phase depends on the masses of both phases and their energy densities. Note that to justify such a picture we have to assume that the mixed phase has sufficiently large volume, so the finite size effects are not significant.

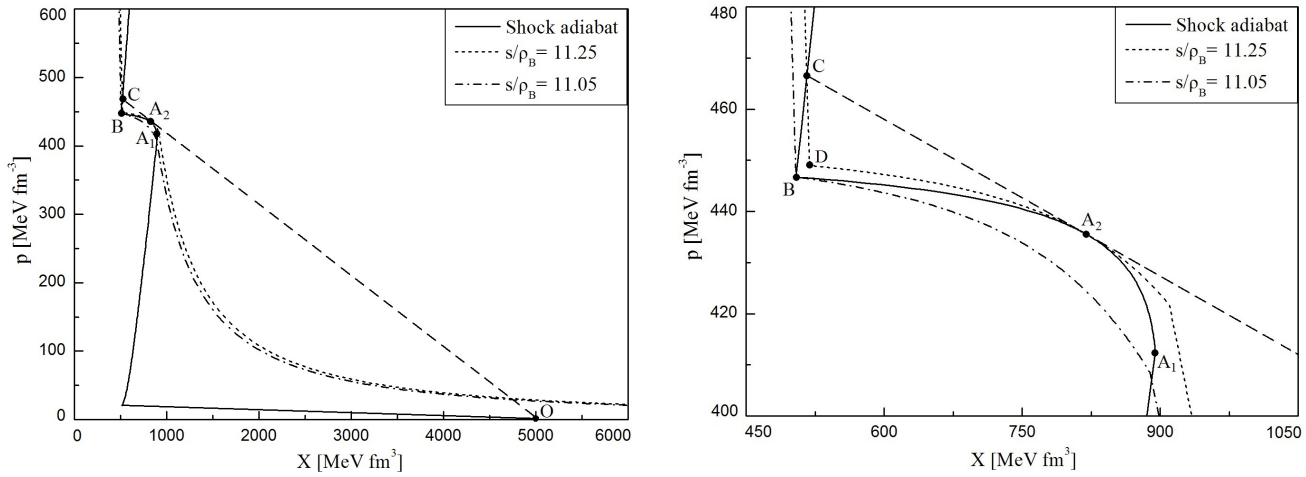


Fig. 5. The compressional shock adiabat OA_1A_2BC (solid curve) in the $X-p$ plane found in [6,7]. It is calculated for the EoS with first-order phase transition discussed in the text. The segments OA_1, A_1B, and BC of the adiabat correspond to the hadronic, mixed and new phases (see below for its interpretation), respectively. Shock transitions into the region of states A_2BC are mechanically unstable. Hence the segment A_2BC should be replaced by the generalized shock adiabat taken from [6,7]. The tangent point A_2 to the shock adiabat (see the dashed line) is the Chapman-Jouguet point [61]. The dotted and dash-dotted curves show the Poisson adiabats with values of entropy per baryon specified in the legend. The right panel shows more details inside the mixed phase region. For more explanations see the text.

Above we discussed a static picture, but the question is whether the condition of constant pressure can be achieved in central nuclear collisions at $\sqrt{s_{NN}} = 4.3 - 4.9$ GeV. To extend this picture to the case of central collisions of heavy ions we refer to the compressional shock model of these collisions [54–59] and its generalization to the mixed phase with the anomalous thermodynamic properties [6, 7, 11, 12]. This model of the collision process, which neglects the nuclear transparency, can be reasonably well justified

at intermediate collision energies per nucleon 1 A GeV $\leq E_{lab} \leq$ 20 A GeV [55–59]. Moreover, the direct comparison of the results of the compressional shock model with those of the three-fluid model [60] made in Ref. [59] demonstrates once more that at laboratory energies up to 30 A GeV this model can be used for quantitative estimates, while at higher energies (up to about 50 A GeV in laboratory frame) it provides a qualitative description only.

The compressional shock model of central nuclear collisions allows one to determine the initial conditions for the subsequent hydrodynamic evolution. The latter are given by the shock adiabat [61], each point of which corresponds to a certain energy of collision (more details can be found in [11,59]). The shock adiabat OA_2BC (see Fig. 5) which was found in [6, 7] shows that in the mixed phase (the segment A_1A_2B in Fig. 5) of the 1-st order phase transition the pressure at the central longitudinal rapidity region practically does not depend on the collision energy. Note, however, that the shock transitions into the states belonging to the segment A_2BC for the shock adiabat OA_2BC of Fig. 5 are mechanically unstable [62, 63] due to anomalous thermodynamic properties of the mixed phase (the segment A_2B) and in this case more complicated flow patters should appear. The latter for the relativistic shock waves were determined in [11,12] and were calculated in [6, 7]. In particular, the shock adiabat region of mixed phase A_2B should be replaced by the the Poisson adiabat [61] A_2D (see the right panel of Fig. 5; here and below the variable $X \equiv \frac{(\epsilon+p)}{\rho_B^2}$ denotes the generalized specific volume [61]). It is remarkable that from the point A_2 to the point D on the Poisson adiabat the pressure changes from about 440 MeV·fm^{-3} to about 450 MeV·fm^{-3}, i.e. the relative change of pressure is about 1/44 or 2.27%. The flow configuration which corresponds to the segment A_2D consists of the compressional shock wave and compressional simple wave moving outwards (see Fig. 6). The shock wave describes the transition from the cold nuclear matter state $(X_0; p_0 = 0)$ (the point O in Fig. 5) to the state $(X_{A_2}; p_{A_2})$, i.e. the tangent point A_2 to the shock adiabat, while the compressional simple wave describes the transformation from the state $(X_{A_2}; p_{A_2})$ to any state $(X; p)$ on the considered segment of the Poisson adiabat with $X_{A_2} \geq X \geq X_D$ and $p_{A_2} \leq p \leq p_D$ (see Refs. [6, 7, 11, 12] for more details). In other words, by increasing the collision energy, at the central rapidity region of the collision one creates the states with higher energy density, but, practically, with the constant pressure. Also due to the fact that the energy density of created dense phase (the phase of massless particles or (PMP) hereafter) is about 10 times higher than the one of the hadron gas [6,7], the major part of energy of a matter formed after the compressional shocks between the states $(X_0; p_0 = 0)$ and $(X_{A_2}; p_{A_2})$ disappear is concentrated right at the central rapidity region of collision. Therefore, just the mixed phase states with practically the same pressure and the same value of entropy per baryon in each 3-dimensional point of the formed matter should define the pattern of its hydrodynamic expansion. Apparently, the hadronic matter which will be born from the mixed phase will be in a full thermal and chemical equilibrium with it. Its further hydrodynamic evolution is out of the scope of the present work, but according to the contemporary paradigm the hadronic matter, including the strange hadrons, born off the mixed phase will remain in the full equilibrium till the moment of CFO.

If the collision energy increases above the point D on the Poisson adiabat, then the matter formed at the central rapidity region of collision will correspond to the segment

DC and the part of mixed phase will gradually decrease vanishing completely at the point C of the shock adiabat. Simultaneously, the role of mixed phase as the explicit thermostat and particle reservoir will be gradually diminished. Counting the discussion above, we can explain the $\gamma_s = 1$ dale seen in the right panel of Fig. 4 by the mixed phase formation at the collision energies $\sqrt{s_{NN}} = 4.3 - 4.9$ GeV and its steady disappearance at $\sqrt{s_{NN}} = 6.3 - 7.6$ GeV together with the corresponding appearance of chemical nonequilibrium of strangeness. Furthermore, such a hypothesis allows one to simultaneously understand the strong increase of the modified Wroblewski factor λ_s within the collision energy interval $\sqrt{s_{NN}} = 2.7 - 7.6$ GeV and the nontrivial collision energy dependence of the γ_s factor at these energies (compare the both panels of Fig. 4).

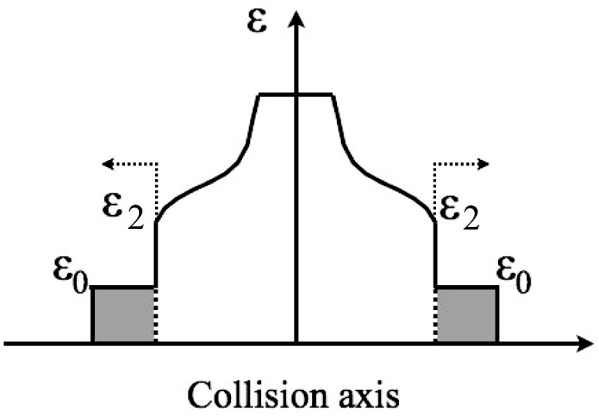


Fig. 6. Sketch of the energy density profile for a central collision of two nuclei (grey areas) that corresponds to a stable flow pattern to the mixed phase region A_2D of Fig. 5. The dashed arrows show the direction of shock propagation in the center of mass frame. Two shocks between the states ε_0 (the point O in Fig. 5) and ε_2 (the point A_2 in Fig. 5) are followed by the compressional simple waves. For more details see the text.

Although it is expected that in QCD there may exist two phase transitions, i.e. deconfinement and chiral symmetry restoration, it is hard to unambiguously identify the nature of phase transition at $\sqrt{s_{NN}} = 4.3 - 4.9$ GeV, since presently there is no reliable information from lattice QCD at high baryonic densities. In Refs. [6,7,10] it was concluded that at these collision energies there may exists the QGP which is probed by the lattice QCD approach. According to our present hypothesis in heavy ion collisions the two phase transitions may be observed. From the discussion above it is clear that at the collision energies $\sqrt{s_{NN}} = 8.8 - 9.2$ GeV there may exist transition to the QGP, i.e. the phase of matter studied by the lattice QCD, and, hence, at the collision energies $\sqrt{s_{NN}} = 4.3 - 4.9$. GeV the transition to QGP is impossible. Thus, the latter collision energy range may correspond to another phase which we call the phase of massless particles (PMP). Although at present the amount of experimental data at the collision energy range $\sqrt{s_{NN}} = 4.9 - 9.2$ GeV is rather limited, we can make an educated guess about its properties. Our guess is based on the EoS of the PMP which was determined

in Refs. [6, 7] from fitting the entropy per baryon s/ρ_B along the shock adiabat [11, 12]. This EoS is similar to the MIT-Bag model [64]

$$p_{PMP} = A_0 T^4 + A_2 T^2 \mu^2 + A_4 \mu^4 - B\,, \tag{9}$$

but the constants $A_0 \simeq 2.53 \cdot 10^{-5}$ MeV^{-3}fm^{-3}, $A_2 \simeq 1.51 \cdot 10^{-6}$ MeV^{-3}fm^{-3}, $A_4 \simeq 1.001 \cdot 10^{-9}$ MeV^{-3}fm^{-3}, and $B \simeq 9488$ MeV fm^{-3} are rather different from what is predicted by the perturbative QCD for massless gluons and (anti)quarks. Despite this fact, an additional condition that the pseudocritical temperature value at zero baryonic density is about 150 MeV was used in the fitting procedure of Ref. [6]. Note that the value $T = 150$ MeV is in agreement with the lattice QCD data [65].

In Ref. [6] the difference of coefficients A_0, A_2 and A_4 from the ones of perturbative QCD A_0^{pQCD}, A_2^{pQCD}, and A_4^{pQCD} was interpreted as the T and μ_B dependence of non-perturbative pressure $B_{eff}(T, \mu_B) \equiv B - (A_0 - A_0^{pQCD})T^4 - (A_2 - A_2^{pQCD})T^2\mu^2 - (A_4 - A_4^{pQCD})\mu^4$ at high baryonic densities. Then the pressure (9) can be rewritten as $p = A_0^{pQCD}T^4 + A_2^{pQCD}T^2\mu^2 + A_4^{pQCD}\mu^4 - B_{eff}$. This was a way to avoid the contradiction with perturbative QCD. However, now, in accordance with the hypothesis of two phase transitions, one can consider Eq. (9) differently, namely as a source of information about the PMP which is formed at the collision energies 4.9 GeV $< \sqrt{s_{NN}} <$ 8.8 GeV.

Recall that the EoS for massless bosons and fermions (with the chemical potential μ) has the form [66]

$$p_{massless\ gas} = \frac{\pi^2 N_{dof}^{eff}}{90}\, T^4 + \frac{N_f^{eff}}{12}\, T^2\mu^2 + \frac{N_f^{eff}}{24\,\pi^2}\, \mu^4\,, \tag{10}$$

where the number of the massless degrees of freedom $N_{dof}^{eff} = N_{bos}^{eff} + \frac{7}{4}N_f^{eff}$ is given in terms of degeneracy factors of massless bosons N_{bos}^{eff} and massless (anti)fermions N_f^{eff}. Comparing the coefficients of powers of temperature in Eqs. (9) and (10) one can estimate the number of the massless degrees of freedom of this phase N_{dof}^{eff} from the coefficient A_0. Then one obtains the number of massless boson and fermion degrees of freedom $N_{dof}^{eff} = \frac{90}{\pi^2}\, A_0\hbar^3 \simeq 1770$, where we used the Planck constant $\hbar$ in order to get a dimensionless value of A_0. Note that N_{dof}^{eff} is essentially larger than the number of massless degrees of freedom of QCD (the total degeneracy of gluons, quarks and antiquarks), but it is comparable to the total number of spin-isospin configurations of known hadronic states [67]. Assuming that fermions have the baryonic charge ± 1, one can use the coefficient A_2 to estimate the number of massless fermionic and antifermionic degrees of freedom $N_f^{eff} = 12\, A_2\hbar^3 \simeq 141$, then one finds that it is still far larger than the expected number of quarks and antiquarks. Also one can use the coefficient A_4 to get the number of massless fermionic and antifermionic degrees of freedom $\widetilde{N}_f^{eff} = 24\pi^2\, A_4\hbar^3 \simeq 1.82$ which is inconsistent with $N_f^{eff} \simeq 141$ found from the coefficient A_2. Clearly, it would be a great surprise, if the coefficients A_2 and A_4 of Eq. (9) would completely agree with the corresponding coefficients in Eq. (10). Hence, we conclude that interaction between the constituents of PMP may differ from the simple bag model parameterization. Nevertheless, our hypothesis is that the PMP consist of non-strange hadronic states with the mass m_{eff} which is much smaller than T, i.e. $m_{eff} \ll T$. In this case the PMP can

be considered as the hadronic state with the restored unitary symmetry. Our hypothesis on the PMP existence is strongly supported by the results of the microscopic model Parton-Hadron-String Dynamics (PHSD) [68, 69] which show that at the vicinity of the collision energy $\sqrt{s_{NN}} \simeq 7$ GeV the effects of baryonic and partonic mass reduction, i.e. the effects of chiral symmetry restoration in the hadronic phase, are very strong.

The question about existence of almost massless strange hadrons in the PMP cannot be answered at the moment with high confidence, i.e. now it is unclear whether the unitary symmetry in PMP is restored completely or in the non-strange sector only. However, looking at the γ_s peaks at $\sqrt{s_{NN}} = 3.8$ GeV and $\sqrt{s_{NN}} = 7.6$ GeV in the right panel of Fig. 4 one may guess that the same mechanism of the strangeness enhancement may be responsible for them, while this mechanism disappears at $\sqrt{s_{NN}} \geq 8.8$ GeV due to the formation of quark-gluon bags with the Hagedorn mass spectrum. Therefore, if in the hadronic phase, i.e. at $\sqrt{s_{NN}} < 4.3$ GeV the strange hadrons are massive, then we believe it is reasonable to assume that in the PMP they are massive too. Although the PHSD microscopic model predicts an essentially weaker reduction of the constituent strange quark compared to the mass of constituent u- and d-quarks [69], we believe that the questions of whether and how the masses of strange hadrons in the PMP are reduced compared to the vacuum values, will have to be answered experimentally on the accelerators of new generation, i.e. NICA JINR and FAIR GSI.

It is interesting that a long time ago an existence of the hadronic phase with abundant number of baryon-antibaryon pairs was discussed in Ref. [70]. In this model the nonlinear interaction of scalar meson provides an essential reduction of baryonic masses and generates an additional solution to the usual hadronic matter which in Ref. [70] is called as the abnormal matter. Similar additional solutions for the self-interacting mesonic fields are also discussed in [71–73]. It is intriguing, however, that some thermodynamic parameters of the normal/abnormal matter are close to our findings. For example, on the isotherm $T = 148$ MeV shown in Fig. 3 of [70] the maximal pressure of the usual hadronic matter (normal state according to Ref. [70]) is about 420 MeV$\cdot$fm^{-3}. Just compare it with the pressure of point A_1 on the boundary of hadronic and mixed phases in Fig. 5. On the other hand, from Fig. 3 of [70] one can see that along the isotherm $T = 148$ MeV the abnormal matter can acquire higher values of pressure which are comparable to the ones shown in Fig. 5 of this work for the compressional and generalized shock adiabats.

Of course, the existence of PMP with nearly massless non-strange hadrons is not the only possibility. Another possibility could be a presence of tetraquark condensate, which may generate two 1-st order chiral phase transitions [74]. One more possibility could be an existence of the quarkyonic matter [75], which has an appropriate collision energy range. Hopefully, the nature and properties of the PMP will be studied at the accelerators NICA JINR and FAIR GSI. However, despite of its origin, if at high temperatures one takes the EoS (9) literally, then one apparently faces a contradiction with the lattice QCD thermodynamics. Indeed, if one fixes μ and increases T, then despite of the large value of constant pressure B in Eq. (9) at high temperatures the pressure of PMP p_{PMP} will exceed the pressure of massless (anti)quarks and gluons. The first possibility to avoid such a contradiction is to claim that the PMP pressure (9) can be used just in the vicinity of the phase transition, since it does not correctly account for interaction of constituents at higher energy density. Basically we agree with this statement, but, in addition, we consider a possibility to get rid of the discussed contradiction with lattice

QCD on a physical ground.

Phase of massless particles with relativistic hard-core repulsion

If, according to our hypothesis, the PMP consists of hadrons, then one cannot ignore their hard-core repulsion. Nowadays there are many articles discussing various applications of the hard-core repulsion in high energy nuclear physics [8, 9, 14–18, 43, 44, 76–78], however, the rigorous approach to relativistic treatment of Lorentz contraction of rigid spheres was developed in Refs. [43, 44]. The ultra-relativistic limit of Lorentz contracted rigid spheres analyzed in [44] shows that in contrast to the non-relativistic case the EoS with relativistic Van der Waals hard-core repulsion is causal at high pressures, i.e. its speed of sound does not exceed the speed of light.

Our suggestion to avoid a contradiction with the lattice QCD thermodynamics is to account for the Lorentz contraction of rigid spheres in the PMP pressure (9) in the spirit of Ref. [44]. For simplicity we consider the Boltzmann limit of a one component gas, i.e. for equal masses of bosons and (anti)fermions and the same hard-core radius R_0. Note that such a simplification is in line with the main property of PMP that particle masses are negligible compared to system temperature and simultaneously it provides us with a qualitatively correct solution of this complicated task. The pressure of the Lorentz contracted rigid spheres $p_{rel}(T,\mu)$ having the temperature T, the chemical potential μ and the relativistic excluded volume per particle $v(\mathbf{k}_1,\mathbf{k}_2)$ is given by a solution of the system [44]

$$p_{rel}(T,\mu) = g\, F_{rel}(T,\mu,p_{rel})\,, \tag{11}$$

$$F_{rel}(T,\mu,p) \equiv \frac{T}{\rho_{th}(T)}\exp\left[\tfrac{\mu}{T}\right]\int \frac{d\mathbf{k}_1}{(2\pi)^3}\frac{d\mathbf{k}_2}{(2\pi)^3}\,\exp\left[-\tfrac{v(\mathbf{k}_1,\mathbf{k}_2)\,p+E(k_1)+E(k_2)}{T}\right], \tag{12}$$

$$\rho_{th}(T) = \int \frac{d\mathbf{k}}{(2\pi)^3}\exp\left[-\tfrac{E(k)}{T}\right], \tag{13}$$

where m is the mass of hadron, g is its degeneracy factor, $\rho_{th}(T)$ denotes the thermal density of particles per single degree of freedom, $E(k)=\sqrt{k^2+m^2}$ is relativistic energy of particle having the 3-momentum $\vec{k}$ and μ is its baryonic chemical potential. In the ultra-relativistic limit the relativistic excluded volume per particle $v(\mathbf{k}_1,\mathbf{k}_2)$ can be cast as [44]

$$v(\mathbf{k}_1,\mathbf{k}_2)\approx\frac{v_0}{2}\left[\frac{m}{E(\mathbf{k}_1)}+\frac{m}{E(\mathbf{k}_2)}\right]\left[1+\cos^2\left(\frac{\Theta_v}{2}\right)\right]^2+\frac{3\,v_0}{2}\sin\left(\Theta_v\right)\,, \tag{14}$$

where the non-relativistic proper volume of particle with the hard-core radius R_0 is $v_0=\frac{4}{3}\pi R_0^3$. Eq. (13) is valid for $0\le\Theta_v\le\frac{\pi}{2}$; to use it for $\frac{\pi}{2}\le\Theta_v\le\pi$ one has to make a replacement $\Theta_v\longrightarrow\pi-\Theta_v$ in (13). The coordinate system is chosen in such a way that the angle Θ_v between the 3-vectors of particles' momenta $\mathbf{k}_1$ and $\mathbf{k}_2$ coincides with the usual spherical angle Θ of spherical coordinates (for more details see Appendix A in [44]). For definiteness, the OZ-axis of the momentum space coordinates of the second particle is chosen to coincide with the 3-vector of the momentum $\mathbf{k}_1$ of the first particle.

It is evident that the volume $v(\mathbf{k}_1, \mathbf{k}_2)$ strongly depends not only on particle momenta, but on the angle between them. Due to this property at high pressure p_{rel} the contribution of configurations with larger volume $v(\mathbf{k}_1, \mathbf{k}_2)$ are suppressed and, hence, the main contribution to the double integral in Eq. (11) is given by the configurations with the minimal value of relativistic excluded volume. It is remarkable that with an accuracy of about 7% the ultra-relativistic expression (14) recovers the excluded volume of two non-relativistic rigid spheres [44] and, therefore, it can be safely used at low particle densities too.

Using the pressure of Lorentz contracted rigid spheres (11), for $m \ll T$, one can generalize EoS (9) to high energy densities as

$$\begin{aligned} \tilde{p}_{PMP} &\simeq T\pi^2(A_0 - 2A_2)F_{rel}(T, 0, \tilde{p}_{PMP}) + T\pi^2 A_2[F_{rel}(T, \mu, \tilde{p}_{PMP}) \\ &+ F_{rel}(T, -\mu, \tilde{p}_{PMP})] - B - \left(\frac{A_2}{12} - A_4\right)\mu^4 . \end{aligned} \tag{15}$$

The first term on the right hand side of Eq. (15) corresponds to the Boltzmann gas of chargeless particles, while the second and third ones correspond to the Boltzmann gas of particles with charges +1 and -1, respectively. Expanding the exponents $\exp(\pm\mu/T)$ which are staying on the right hand side of (15) up to terms $(\mu/T)^6$, one can readily check that for $m \ll T$ and $\frac{v_0\,\tilde{p}_{PMP}}{T} \ll 1$ the right hand side of (15) recovers the one of Eq. (9). The term $\frac{A_2\,\mu^4}{12}$ on the right hand side of (15) "compensates" an extra contribution coming from the expansion of fermionic exponents $\exp(\pm\mu/T)$. It is easy to verify that for massless particles and a zero value of hard-core radius R_0 the T and μ dependent terms of pressures (9) and (15) differ from each other by less than 10% for $\left|\frac{\mu}{T}\right| \leq 2.8$ and any T.

Apparently, Eq. (15) is not a unique way to extrapolate the PMP pressure (9) to high energy densities, but, besides the fact that the pressure (15) is one of the simplest possibilities, one can also check that for $T \geq 137.1$ MeV and $m \ll T$ it has only a single positive solution $\tilde{p}_{PMP}(T, \mu) > 0$ for any value of $\dfrac{\mu}{T}$. Therefore, we believe that Eq. (15) is well suited for demonstrating how the Lorentz contracted relativistic excluded volume can modify the PMP pressure at high energy densities. A sufficient condition for an existence of a single positive solution $\tilde{p}_{PMP}(T, \mu)$ of (15) can be found as follows. For the fixed values of μ and T with the restriction $m \ll T$ one can solve Eq. (15) graphically. Noting that the right hand side of (15) is a monotonously decreasing function of the variable $\tilde{p}_{PMP}$ due to excluded volume effect, one can conclude that such a function can have a single intersection with the straight line $p = \tilde{p}_{PMP}$, i.e. with the left hand side of (15), if at the point $p = 0$ the inequality

$$\begin{aligned} &T\pi^2(A_0 - 2A_2)F_{rel}(T, 0, 0) + T\pi^2 A_2\left[F_{rel}(T, \mu, 0) + F_{rel}(T, -\mu, 0)\right] \\ &-B - \left(\frac{A_2}{12} - A_4\right)\mu^4 > 0 , \end{aligned} \tag{16}$$

is obeyed.

Assuming that the condition (16) is obeyed, we consider the asymptotic behavior of the pressure (15) for two cases, namely high T limit and high μ limit. Apparently, both of them correspond to a high pressure limit and, therefore, the bag pressure B and the

last term on the right hand side of Eq. (15) can be neglected. Applying the results of Ref. [44] to Eqs. (12), one can easily show that in the limit $T \to \infty$ the dimensionless variable $z \equiv \frac{2m\, v_0\, p_{rel}}{T^2} \to Const < \infty$. Using this result for the pressure (15), in the limit $T \to \infty$ and finite values of μ one can find

$$\tilde{p}_{PMP}(T,\mu) \to \left[\frac{\pi^2 A_0 + 2\pi^2 A_2(\cosh\left[\frac{\mu}{T}\right]-1)}{v_0^2}\right]^{\frac{1}{3}} T^2\, f(m)\,, \tag{17}$$

where $f(m) \sim O(1)$ is a slowly decreasing dimensionless function of hadronic mass m. The effective number of degrees of freedom now is $[\pi^2 A_0 \hbar^3]^{\frac{1}{3}} \simeq 12.4$. Moreover, the temperature dependence of pressure (17) is essentially weaker than the one for massless quarks and gluons (see Eq. (10)).

In the limit of fixed T and $\mu \to \infty$ one finds for Eqs. (11) and, similarly, for (15) that [44]

$$\tilde{p}_{PMP}(T,\mu) \to \frac{\mu^2}{32\, m\, v_0}\ , \tag{18}$$

the pressure of relativistic hard-spheres does not depend on the number of degrees of freedom at all and its μ dependence is again essentially weaker than μ^4 dependence of massless (anti)quarks. Therefore, these two examples show that the Lorentz contraction of relativistic hard-spheres, in principle, is able to resolve the problem of high energy density extrapolation of PMP EoS (9) in such a way that it does not contradict to QCD phenomenology.

Conclusions

In this work we perform a thorough inspection of the irregularities of thermodynamic quantities observed at CFO and discuss the possible signals of two QCD phase transitions. The most remarkable irregularities include two sets of correlated quasi-plateaus found in [6, 7] which are located at the collision energy ranges $\sqrt{s_{NN}} \simeq 3.8 - 4.9$ GeV and $\sqrt{s_{NN}} \simeq 7.6 - 9.2$ GeV, and two peaks of trace anomaly δ observed at the maximal energy of each set of quasi-plateaus. Using the most advanced version of the hadron resonance gas model which allows one to safely go beyond the standard Van der Waals approximation, here we found two strong peaks of the baryonic charge density located exactly at the collision energies of the trace anomaly peaks, i.e. at $\sqrt{s_{NN}} = 4.9$ GeV and $\sqrt{s_{NN}} = 9.2$ GeV. The usage of the NHRGM which is not restricted by the Van der Waals approximation was necessary, since at the mentioned peaks the baryonic charge density is high and corresponds to $1.25-1.4$ values of the normal nuclear density $\rho_0 = 0.16$ fm^{-3}. Moreover, during the fitting even higher values of baryonic charge density were analyzed.

In addition in this work we closely studied the collision energy dependence of the ratio of total number of strange quarks and antiquarks to the number of non-strange quarks and antiquarks (a modified Wroblewski factor λ_s) and the strangeness suppression factor γ_s. With the help of NHRGM we find a sizable jump of the λ_s factor, when the collision energy increases from $\sqrt{s_{NN}} = 4.3$ GeV to $\sqrt{s_{NN}} = 4.9$ GeV, while at the collision

energies above $\sqrt{s_{NN}} = 7.6$ GeV we observe a saturation of the λ_s factor. Similarly to previous findings [8,9,15] we observe rather complicated energy dependence of γ_s factor: at $\sqrt{s_{NN}} = 3.8$ GeV and $\sqrt{s_{NN}} = 7.6$ GeV there exist two maxima, while at $\sqrt{s_{NN}} = 4.9$ GeV and at $\sqrt{s_{NN}} > 8.7$ GeV the strangeness seems to reach a chemical equilibrium.

Since the low energy set of quasi-plateaus along with the trace anomaly peak at $\sqrt{s_{NN}} = 4.9$ GeV are unambiguously explained by the anomalous thermodynamic properties of mixed phase of the 1-st order phase transition formed at $\sqrt{s_{NN}} = 4.3 - 4.9$ GeV [6,7], we conclude that other irregularities observed at $\sqrt{s_{NN}} = 4.9$ GeV, i.e. the peak of baryonic charge density, the λ_s factor jump and the strangeness equilibration can be the other signals of this phase transition. In this work we give a straightforward explanation to the strangeness equilibration at $\sqrt{s_{NN}} = 4.9$ GeV and at $\sqrt{s_{NN}} > 8.7$ GeV. Based on the unique thermostatic properties of Hagedorn mass spectrum we follow Ref. [15] and suggest that at $\sqrt{s_{NN}} > 8.7$ GeV the formation of quark-gluon bags with the exponential mass spectrum forces the hadrons born at the moment of hadronization to be in a full thermal and chemical equilibrium with the bags. Similarly, in this work we notice that under the condition of the constant external pressure any mixed phase of the 1-st order phase transition is an explicit thermostat and explicit particle reservoir and, hence, anything born out of it should be in a full thermal and chemical equilibrium with the mixed phase. Since the mixed phase EoS employed in Refs. [6,7], indeed, leads to an approximate collision energy independence of initial pressure of a system formed in the collision process, we came to a natural conclusion that the formation of mixed phase at $\sqrt{s_{NN}} = 4.9$ GeV is responsible for the chemical equilibration of strangeness at this energy. Thus, the explicit thermostatic properties of the mixed phase cause an appearance of the strangeness equilibrium dale at $\sqrt{s_{NN}} = 4.9$ GeV. On the other hand, due to an absence of an alternative explanation of such a dale, its appearance, in turn, is an independent and strong argument in favor of the mixed phase formation at this collision energy.

As it is argued here and in Refs. [6,7] the above mentioned irregularities observed at the collision energy range $\sqrt{s_{NN}} \simeq 3.8 - 4.9$ GeV are the signals of the 1-st order phase transition, then, according to our hypothesis, a set of similar irregularities found at the collision energies $\sqrt{s_{NN}} \simeq 7.6 - 9.2$ GeV should be associated with another phase transition. Such a hypothesis is supported by the detailed analysis of K^+/π^+ ratio of Ref. [53] and by the one of light nuclei fluctuations of Ref. [13]. In addition to thermodynamic and hydrodynamic signals of phase transition discussed here the work [13] provides us with the fluctuation signal of the 2-nd order phase transition at the vicinity of $\sqrt{s_{NN}} \simeq 8.8 - 9.2$ GeV. Therefore, we argue that the collision energy range $\sqrt{s_{NN}} \simeq 8.8 - 9.2$ GeV may be the nearest vicinity of 3CEP.

The EoS (9) used in [6,7] to model the properties of high density matter formed at the initial stage of collision for the energies $\sqrt{s_{NN}} \simeq 6.3 - 9.2$ GeV provides us with a unique opportunity to reveal the total number of massless bosonic and fermionic degrees of freedom. The found number is about 1770, which is too large for elementary degrees of freedom of QCD, but it has the same order of magnitude as the total number of experimentally known hadronic spin-isospin states. Although, at the moment there is insufficient data to discuss a possible origin of this phase, our hypothesis that such a phase corresponds to a gas of interacting, but almost massless hadrons, is strongly supported by the results of PHSD microscopic model which accounts for the effects of hadronic and

partonic mass reduction in a very similar energy range [68, 69]. Therefore, we explicitly show that, if one accounts for the excluded volume of these hadronic degrees of freedom in a relativistic fashion, then at high energy densities the EoS (9) can be modified in such a way that it does not contradict to the QCD thermodynamics.

The above results and hypotheses are rather speculative, but they reflect the present state of art of heavy ion collision phenomenology, where at the moment there is insufficient experimental and theoretical information right at the most promising regions of the QCD phase diagram. Therefore, we hope that this work will stimulate both theoreticians and experimentalists to study the discussed problems in more details in order to prove or disprove our results.

Acknowledgments. The authors appreciate the valuable comments of E. E. Kolomeitsev, S. N. Nedelko and A. I. Titov. K.A.B., A.I.I., V.V.S. and G.M.Z. acknowledge a partial support from the program "Nuclear matter under extreme conditions" launched by the Section of Nuclear Physics of the National Academy of Sciences of Ukraine. The work of K.A.B. and L.V.B. was performed in the framework of COST Action CA15213 "Theory of hot matter and relativistic heavy-ion collisions" (THOR). K.A.B. is thankful to the COST Action CA15213 for a partial support. V.V.S. acknowledges a partial support by grants from "Fundação para a Ciência e Tecnologia". The work of D.B. was supported in part by the Polish National Centre (NCN) under contract number UMO-2011/02/A/ST2/00306. The work of A.V.T. was partially supported by the Ministry of Science and Education of the Russian Federation, grant No 3.3380.2017/4.6, and by National Research Nuclear University "MEPhI" in the framework of the Russian Academic Excellence Project (contract No 02.a03.21.0005, 27.08.2013).

REFERENCES

1. Stephanov M., Rajagopal K. and Shuryak E. Event-by-event fluctuations in heavy ion collisions and the QCD critical point // Phys. Rev. D — 1999. — V. 60, no. 114028. — P. 1–32 and references therein.

2. NICA White Paper // — 2013. — V. 9.01 and references therein.

3. Lacey R. Indications for a Critical End Point in the Phase Diagram for Hot and Dense Nuclear Matter // Phys. Rev. Lett. — 2015. — V. 114, no. 14. — P. 142301 and references therein.

4. Antoniou N.G., Davis N. and Diakonos F.K., What is the gamma gamma resonance at 750 GeV? — 2016. — arXiv:1607.01326v1 [nucl-th] see a discussion therein.

5. Ladrem M. and Ait-El-Djoudi A., Finite-size effects and scaling for the thermal QCD deconfinementphase transition within the exact color-singlet partition function // Eur. Phys. J. C — 2005. — V. 44, no. 2. — P. 257265.

6. Bugaev K.A., Ivanytskyi A.I., Oliinychenko D.R., Sagun V.V., Mishustin I.N., Rischke D.H., Satarov L.M. and Zinovjev G.M. Thermodynamically Anomalous Regions As A Mixed Phase Signal // Phys. Part. Nucl. Lett. — 2015. — V. 12, no. 2 — P. 238245, arXiv:1405.3575.

7. Bugaev K.A., Ivanytskyi A.I., Oliinychenko D.R., Sagun V.V., Mishustin I.N., Rischke D.H., Satarov L.M. and Zinovjev G.M. Thermodynamically anomalous regions and possible new signals of mixed-phase formation // Eur. Phys. J. A — 2016, — V. 52, no. 6, — P. 175, arXiv:1412.0718.

8. Bugaev K.A., Oliinychenko D.R., Cleymans J., Ivanytskyi A.I., Mishustin I.N., Nikonov E.G. and Sagun V.V. Chemical Freeze-out of Strange Particles and Possible Root of Strangeness Suppression // Europhys. Lett. — 2013, — V. 104,— P. 22002 and references therein.

9. Sagun V.V. Λ-Anomaly in the Hadronic Chemical Freeze-out // Ukr. J. Phys. — 2014, — V. 59, no. 8,— P. 755-763.

10. Bugaev K.A., Sagun V.V., Ivanytskyi A.I., Oliinychenko D.R., Ilgenfritz E.-M., Nikonov E.G., Taranenko A.V. and Zinovjev G.M. New Signals of Quark-Gluon-Hadron Mixed Phase Formation // Eur. Phys. J. A — 2016, — V. 52, — P. 227, arXiv:1510.03099.

11. Bugaev K.A., Gorenstein M.I., Kämpfer B.,Zhdanov V.I. Generalized shock adiabatics and relativistic nuclear collisions // Phys. Rev. D — 1989, — V. 40, — P. 2903.

12. Bugaev K.A., Gorenstein M.I., Rischke D.H. Pion multiplicity in heavy-ion collisions: possible signature of the deconfinement transition // Phys. Lett. B — 1991, — V. 255, — P. 18.

13. Kai-Jia Sun, Lie-Wen Chen, Che Ming Ko and Zhangbu Xu Probing QCD critical fluctuations from light nuclei production in relativistic heavy-ion collisions — 2017. — arXiv:1702.07620v1 [nucl-th].

14. Bugaev K.A., Sagun V.V., Ivanytskyi A.I., Yakimenko I.P., Nikonov E.G., Taranenko A.V., Zinovjev G.M. Hadron Resonance Gas Model for An Arbitrarily Large Number of Different Hard-Core Radii — 2016. — arXiv:1611.07349v2 [nucl-th].

15. Sagun V.V., Bugaev K.A., Ivanytskyi A.I., Yakimenko I.P., Nikonov E.G., Taranenko A.V., Greiner C., Blaschke D.B., Zinovjev G.M. Hadron Resonance Gas Model with Induced Surface Tension — 2017. — arXiv:1703.00049 [nucl-th].

16. Bugaev K.A., Ivanytskyi A.I., Sagun V.V., Nikonov E.G., Zinovjev G.M. Equation of State of Quantum Gases Beyond the Van der Waals Approximation — 2017. — arXiv:1704.06846 [nucl-th].

17. Andronic A., Braun-Munzinger P. and Stachel J. Hadron production in central nucleusnucleus collisions at chemical freeze-out // Nucl. Phys. A — 2006, — V. 722, — P. 167.

18. Bugaev K.A., Oliinychenko D.R., Sorin A.S., Zinovjev G.M. Simple solution to the Strangeness Horn description puzzle // Eur. Phys. J. A — 2013, — V. 49, — P. 30.

19. Rischke D.H., Gorenstein M.I., Stöcker H. and Greiner W. Excluded volume effect for the nuclear matter equation of state // Z. Phys. C — 1991, — V. 51, — P. 485.

20. Carnahan N.F., Starlin K.E. Equation of State for Nonattracting Rigid Spheres // J. Chem. Phys. — 1969, — V. 51, — P. 635.

21. Mansoori G.A., Carnahan N.F., Starling K.E., Leland T. W. Jr. Equation of State for Nonattracting Rigid Spheres // J. Chem. Phys. — 1971, — V. 54, — P. 1523.

22. Hansen J.P., McDonaldI.R. Theory of simple liquids. — Academic, London, 2006.

23. Salacuse J.J., Stell G. Polydisperse systems: Statistical thermodynamics, with applications to several models including hard and permeable spheres // J. Chem. Phys. — 1982, — V. 77, — P. 3714.

24. Klay J.L. et al. (E895 Collaboration) Charged pion production in 2A to 8AGeV central Au+Au Collisions // Phys. Rev. C — 2003, — V. 68, — P. 054905.

25. Ahle L. et al. (E866 Collaboration) Excitation function of K^+ and Π^+ production in Au+Au reactions at 210 AGeV // Phys. Lett. B — 2000, — V. 476, — P. 1.

26. Ahle L. et al. (E866 Collaboration) An excitation function of K and K^+ production in Au+Au reactions at the AGS // Phys. Lett. B — 2000, — V. 490, — P. 53.

27. Pinkenburg C. et al. (E895 Collaboration) Production and collective behavior of strange particles in Au+Au collisions at 28 A GeV // Nucl. Phys. A — 2002, — V. 698, — P. 495.

28. Barrette J. et al. (E877 Collaboration) Proton and pion production in Au+Au collisions at 10.8 AGeV/c // Phys. Rev. C — 2000, — V. 62, — P. 024901.

29. Ahle L. et al. (E802 Collaboration) Proton and deuteron production in Au+Au reactions at 11.6 AGeV/c // Phys. Rev. C — 1999, — V. 60, — P. 064901.

30. Ahle L. et al. (E802 Collaboration) Kaon production in Au+Au collisions at 11.6 AGeV/c // Phys. Rev. C — 1998, — V. 58, — P. 3523.

31. Albergo S. et al. Λ Spectra in 11.6 AGeV/c Au-Au Collisions // Phys. Rev. Lett. — 2002, — V. 88, — P. 062301.

32. Back B.B. et al. (PHOBOS Collaboration) Ratios of Charged Antiparticles-to-Particles near Mid-Rapidity in Au+Au Collisions at $\sqrt{s_{NN}}$ = 130 GeVs // Phys. Rev. Lett. — 2001, — V. 87, — P. 102301.

33. Bearden I.G. et al. (NA44 Collaboration) Particle production in central Pb+Pb collisions at 158 AGeV/c // Phys. Rev. C — 2002, — V. 66, — P. 044907.

34. Afanasiev S.V. et al. (NA49 Collaboration) Energy dependence of pion and kaon production in central Pb+Pb collisions // Phys. Rev. C — 2002, — V. 66, — P. 054902.

35. Afanasiev S.V. et al. (NA49 Collaboration) Energy and centrality dependence of deuteron and proton production in Pb+Pb collisions at relativistic energies // Phys. Rev. C — 2004, — V. 69, — P. 024902.

36. Alt C. et al. (NA49 Collaboration) Energy and centrality dependence of anti-p and p production and the anti-Lambda/anti-p ratio in Pb+Pb collisions between 20/A-GeV and 158/A-Gev // Phys. Rev. C — 2006, — V. 73, — P. 044910.

37. Anticic T. et al. (NA49 Collaboration) Λ and $\bar{\Lambda}$ Production in Central Pb-Pb Collisions at 40, 80, and 158 AGeV // Phys. Rev. Lett. — 2004, — V. 93, — P. 022302.

38. Afanasiev S.V. et al. (NA49 Collaboration) Ξ^- and Ξ^+ production in central Pb+Pb collisions at 158 GeV/c per nucleon // Phys. Rev. B — 2002, — V. 538, — P. 275.

39. Alt C. et al. (NA49 Collaboration) Ω^- and Ω^+ Production in Central Pb+Pb collisions at 40 and 158 AGeV // Phys. Rev. Lett. — 2005, — V. 94, — P. 192301.

40. Antinori F. et al. (NA57 Collaboration) Energy dependence of hyperon production in nucleusnucleus collisions at SPS // Phys. Lett. B — 2004, — V. 595, — P. 68.

41. Antinori F. et al. (NA57 Collaboration) Rapidity distributions around mid-rapidity of strange particles in PbPb collisions at 158 A GeV/c // J. Phys. G — 2005, — V. 31, — P. 1345.

42. Adams J. et al. (STAR Collaboration) Identified Particle Distributions in pp and $Au + Au$ Collisions at $\sqrt{s_{NN}} = 200$ GeV // Phys. Rev. Lett. — 2004, — V. 92, — P. 112301.

43. Bugaev K.A., Gorenstein M.I., Stöcker H., Greiner W. Van der Waals Excluded Volume Model for Lorentz Contracted Rigid Spheres // Phys. Lett. B — 2000, — V. 485, — P. 121.

44. Bugaev K.A. Van-der-Waals Gas EOS for the Lorentz Contracted Spheres // Nucl. Phys. A — 2008, — V. 807, — P. 251.

45. Wroblewski A.K. On the Strange Quark Suppression Factor in High Energy Collisions // Acta Phys. Pol. B — 1985, — V. 16, — P. 379.

46. Rafelski J. Strange anti-baryons from quark-gluon plasma // Phys. Lett. B — 1991, — V. 262, — P. 333.

47. Bugaev K.A., Oliinychenko D.R., Ivanytskyi A.I., Cleymans J., Mironchuk E.S., Nikonov E.G., Taranenko A.V., Zinovjev G.M. Separate Chemical Freeze-Outs of Strange and Non-Strange Hadrons and Problem of Residual Chemical Non-Equilibrium of Strangeness in Relativistic Heavy Ion Collisions // Ukr. J. Phys. — 2016, — V. 61, — P. 659.

48. Hagedorn R. Statistical thermodynamics of strong interactions at high energies // Nuovo Cim. Suppl. — 1965, — V. 3, — P. 147.

49. Moretto L.G., Bugaev K.A., Elliott J.B., Phair L. Hagedorn Thermostat // Europhys. Lett. — 2006, — V. 76, — P. 402.

50. Beitel M., Gallmeister K., Greiner C. Thermalization of Hadrons via Hagedorn States // Phys. Rev. C — 2014, — V. 90, — P. 045203, arXiv:1402.1458.

51. Beitel M., Gallmeister K., Greiner C. Equilibration of hadrons in HICs via Hagedorn States // J. Phys. Conf. Ser. — 2016, — V. 668, — P. 012057.

52. Beitel M., Greiner C., Stoecker H. Fast dynamical evolution of a hadron resonance gas via Hagedorn states // Phys. Rev. C — 2016, — V. 94, — P. 021902.

53. Nayak J.K., Banik S., Alam J. The "horn" in the kaon-to-pion ratio // Phys. Rev. C — 2010, — V. 82, — P. 024914.

54. Galitskij V.M., Mishustin I.N. The influence of a phase transition on the shock wave dynamics in nuclear matter // Phys. Lett. B — 1978, — V. 72, — P. 285.

55. Stöcker H., Graebner G., Maruhn J.A., Greiner W. Hot, dense hadronic and quark matter in relativistic nuclear collisions // Phys. Lett. B — 1980, — V. 95, — P. 192.

56. Kämpfer B. Phase transitions in dense nuclear matter and consequences for neutron stars // J. Phys. G — 1983, — V. 9, — P. 1487.

57. Stöcker H., Greiner W. High energy heavy ion collisionsprobing the equation of state of highly excited hardronic matter // Phys. Rep. — 1986, — V. 137, — P. 277.

58. Barz H.W., Csernai L.P., Kämpfer B., Lukacs B. Stability of detonation fronts leading to quark-gluon plasma // Phys. Rev. D — 1985, — V. 32, — P. 115.

59. Merdeev A.V., Satarov L. M., Mishustin I. N. Hydrodynamic modeling of the deconfinement phase transition in heavy-ion collisions in the NICAFAIR energy domain // Phys. Rev. C — 2011, — V. 84, — P. 014907.

60. Ivanov Yu. B., Russkikh V. N., Toneev V. D. Relativistic heavy-ion collisions within three-fluid hydrodynamics: Hadronic scenario // Phys. Rev. C — 2006, — V. 73, — P. 044904.

61. Landau L.D., Lifshitz E.M. Fluid Mechanics. — Pergamon, New York, 1979.

62. Zel'dovich Y.B., Raiser Y.P. Physics of shock waves and high temperature hydrodynamic phenomena. — Academic, New York, 1967.

63. Rozhdestvensky B.L., Yanenko N.N. Systems of Quasi-Linear Equations. — Nauka, Moscow, 1978.

64. Chodos A. et al. New extended model of hadrons // Phys. Rev. D — 1974, — V. 9, — P. 3471.

65. Aoki Y. et al. The QCD transition temperature: Results with physical masses in the continuum limit // Phys. Lett. B — 2006, — V. 643, — P. 46.

66. Chin S.A. Transition to hot quark matter in relativistic heavy-ion collision // Phys. Lett. B — 1978, — V. 78, — P. 552.

67. Particle Data Group // Phys. Lett. B — 2004, — V. 591, — P. 1.

68. Cassing W., Palmese A., Moreau P., Bratkovskaya E. L. Chiral symmetry restoration versus deconfinement in heavy-ion collisions at high baryon density // Phys. Rev. C — 2016 — V. 93, — P. 014902.

69. Palmese A. et. al.Chiral symmetry restoration in heavy-ion collisions at intermediate energies // Phys. Rev. C — 2016 — V. 94, — P. 044912.

70. Glendenning N.K. Hot metastable state of abnormal matter in relativistic nuclear field theory // Nucl. Phys. A — 1987 — V. 469, — P. 600.

71. Garpman S.I.A., Glendenning N.K., Karant Y.J. Thermodynamic behavior of non-strange baryonic matter // Nucl. Phys. A — 1979 — V. 322, — P. 382.

72. Theis J. et al. Phase transition of the nucleon-antinucleon plasma in a relativistic mean-field theory // Phys. Rev. D — 1983 — V. 28, — P. 2286.

73. Nakai T., Takagi S. Influence of the $N^*(1470)$ to Density Isomer and a Phase Transition of the Baryon-Antibaryon Plasma at Finite Temperatures // Prog. Theor. Phys. — 1984 — V. 71, — P. 1118.

74. Pisarski R.D., Skokov V.V. How tetraquarks can generate a second chiral phase transition // Phys. Rev. D — 2016 — V. 94, — P. 054008.

75. Andronic A. et al. Hadron production in ultra-relativistic nuclear collisions: Quarkyonic matter and a triple point in the phase diagram of QCD // Nucl. Phys. A — 2010 — V. 837, — P. 65.

76. Lattimer J.M., Swesty F.D. A Generalized equation of state for hot, dense matter // Nucl. Phys. A — 1991 — V. 535, — P. 331.

77. Shen L.H., Toki H., Oyamatsu K., Sumiyoshi K. Relativistic equation of state of nuclear matter for supernova and neutron star // Nucl. Phys. A — 1998 — V. 637, — P. 435.

78. Typel S. Variations on the excluded-volume mechanism // Eur. Phys. J. A — 2016 — V. 52, — P. 16.